

1 **Quantifying the relationships between environmental factors and**
2 **accumulated tornado energy on the most prolific days in the largest**
3 **“outbreaks”**

4 Zoe Schroder and James B. Elsner*

5 *Florida State University, Tallahassee, Florida*

6 *Corresponding author address: Zoe Schroder, Department of Geography, Florida State University,

7 113 Collegiate Loop, Tallahassee, FL 32301.

8 E-mail: zms17b@my.fsu.edu

ABSTRACT

9 Outbreaks over consecutive days with many tornadoes are typically associ-
10 ated with specific regional scale environmental factors. To quantify the re-
11 lationship between environmental factors and tornado activity, the authors
12 examine big days in the largest outbreaks. They identify the largest groups
13 across space and time and analyze the days within these groups that have
14 at least ten tornadoes (big days). A climatology of the big days shows that
15 they occur most often during April, May, and June across the central United
16 States. Then, defining accumulated tornado energy (ATE) as a metric of big
17 day severity, they statistically examine how this metric is related to environ-
18 mental factors including convective available energy and shear using a regres-
19 sion model. They find an upward trend in per big-day outbreak ATE of 7%
20 [(2.5%, 12%), 95% UI] per annum and an increase in ATE of 83% [(23%,
21 170%), 95% UI] for every $10 \text{ m}^2 \text{ s}^{-2}$ increase in the magnitude of bulk shear.
22 Further, they find an increase of 49% [(18%, 87%), 95% UI] for every 1000
23 J kg^{-1} increase in CAPE. Residuals from the regression model shows no re-
24 gional difference in where the model over predicts ATE and where the model
25 under predicts ATE. However, the number of tornadoes per unit area is larger
26 on big days where the model under predicts ATE.

27 **1. Introduction**

28 Tornado outbreaks pose a large risk for significant damage and casualties. For example, the
29 April 27, 2011 outbreak produced 199 tornadoes. It resulted in 316 fatalities, more than 2700
30 injuries, and insured losses that exceeded \$11 billion (Knupp et al. 2014). The vast majority of
31 tornado-related fatalities occur in outbreaks (Galway 1977; Schneider et al. 2004; Fuhrmann et al.
32 2014). In fact, three-fourths of all fatalities occur on days with the most tornadoes within a large
33 outbreak.

34 The climatology of tornado outbreaks is well documented. Outbreaks vary by location, sea-
35 son, and intensity. In general, outbreaks occur east of the Rocky Mountains and west of the
36 Appalachian Mountains (Dean 2010) and are most common in the central and southeastern part of
37 the country with the frequency of occurrence in those areas varying by season. Tornado outbreaks
38 occur most often during April, May, and June (Galway 1977; Dean 2010). In these months, the
39 majority of outbreaks occur across the Central Plains and the Southeast. Outbreaks become less
40 common in the Southeast and the Southern Plains during the summer months as a result of the
41 northern migration of the jet stream (Concannon et al. 2000). Outbreaks are largely confined to
42 the Southeast during the late fall and winter months (Dean 2010). For example, the November 23,
43 2004 outbreak extended from Texas to Florida and Georgia. It produced 76 tornadoes resulting in
44 40 casualties.

45 Missing from these studies is a quantification of the relationship between environmental factors
46 and collective tornado activity. Specifically, how much convective energy is needed, on average,
47 to produce a 25% increase in tornado activity? Tornado environments have been studied locally
48 using proximity soundings and local weather stations. A proximity sounding is a measure of
49 atmospheric variables such as temperature, pressure, and winds for a specific location and time.

50 These studies have identified environmental factors important to the development of tornadoes
51 such as convective available potential energy (CAPE), speed and directional wind shear, and low
52 cloud-base heights (Brooks et al. 1994; Jackson and Brown 2009; Brown 2002; Craven et al.
53 2002). The amount of CAPE and wind shear varies by event and geographic region. A tornadoes
54 can form in low CAPE with high shear environments and high CAPE with low shear environments
55 (Johns et al. 1993; Korotky et al. 1993; Brooks et al. 1994). Here we are interested in *by how much*
56 tornado activity changes with a unit change in CAPE controlling for wind shear.

57 The objective of the present study is to quantify the extent to which environmental factors mod-
58 ulate collective tornado activity. We first identify the biggest days in the largest groups. We then
59 determine which environmental factors, individually and interactively, best explain cumulative
60 tornado activity. The metric of cumulative activity is accumulated tornado energy and the environ-
61 mental variables we consider include convective available potential energy, convective inhibition,
62 helicity, and bulk shear. The paper is outlined as follows. In section 2, we describe the method
63 we use to define tornado groups, and we compare the resulting list of significant large groups with
64 previous lists of significant outbreaks. In section 3, we describe some of the spatial and temporal
65 characteristics of the biggest days in the largest groups. In section 4, we introduce the metric of
66 accumulated tornado energy (ATE). In section 5, we quantify the relationship between ATE and
67 the environmental variables using regression models. In section 6, we provide a summary and list
68 the main conclusions.

69 **2. Tornado Groups**

70 A tornado can occur as a single isolated event or as one of several to dozens within an outbreak.
71 The American Meteorological Society formally defines a tornado outbreak as “multiple tornado
72 occurrences associated with a particular synoptic-scale system” (American Meteorological Society

73 cited 2018). A tornado outbreak can occur over a time span ranging from as short as an hour to
74 as long as several days. Less formally, it is commonly understood that an outbreak is a group
75 of several to hundreds of tornadoes that occur within a relatively short time scale and over a
76 limited geographic region (Malamud et al. 2016). Here we focus on tornado groups rather than on
77 individual tornadoes because tornado groups have a spatial and temporal extent that is associated
78 with synoptic-scale environmental parameters. We refer to them as a group rather than an outbreak
79 since we make no attempt to associate them with a particular synoptic-scale system (e.g., an extra-
80 tropical cyclone).

81 *a. Method to group tornadoes*

82 We obtain tornado data from the Storm Prediction Center’s extensive tornado record ([https://](https://www.spc.noaa.gov/wcm/#data)
83 www.spc.noaa.gov/wcm/#data). Date, time, and location of each tornado are used to delineate
84 groups of tornadoes. The data are subset to include only tornadoes that occur from 1994 to 2017
85 in the contiguous United States. The start year of 1994 marks the beginning of the extensive use
86 of the WSR-88D radar. There are 29,372 tornadoes over this period of record.

87 We first project the geographic coordinates of the tornado locations using a Lambert Conic
88 Conformal projection for the contiguous United States. The origin of the projection is situated
89 in eastern Kansas at 39 degrees North and 96 degrees West. Then for a given tornado location
90 i , we compute the Euclidean distance (d_{ij}) as the difference between location i and the location
91 of tornado j . Similarly we compute a time difference (t_{ij}) between the time of tornado i and the
92 time of tornado j . The space difference has units of meters and the time difference has units
93 of seconds. The space difference is divided by ten so the magnitude is commensurate with the
94 corresponding time difference under the assumption that, on average, thunderstorms move at ten
95 meters per second. For every tornado pair, the space and time differences are added to give a total

96 space-time difference (Eq. 1).

$$\delta_k = d_{ij} + t_{ij}, \quad (1)$$

97 where $k = n(n + 1)/2$ indexes the unique tornado pairs and n is the number of tornadoes.

98 Next, the set of k space-time differences (δ_k) is used to place each tornado into a group. If tor-
99 nado i is in close proximity to tornado j based on a small δ_k , then the two tornadoes are considered
100 in the same group. Grouping is done using the single-linkage method whereby the two tornadoes
101 with the smallest δ_k are grouped first. The first group is given a space-time difference based on the
102 centroid (average) of the space-time differences of the two tornadoes. Then the two tornadoes (or
103 the first tornado group centroid and another tornado) with the next smallest δ_k are grouped second.
104 The procedure continues by grouping tornado pairs, group-tornado pairs, and group-group pairs
105 until there is a single large group. The grouping is done with the `hclust` function from the **stats**
106 package and it produces the same result as the ST-DBSCAN algorithm (Birant and Kut 2007).

107 Our interest centers on groups that are not too small (e.g., a family of tornadoes from a single
108 supercell) and not too large (e.g., all tornadoes during a year). So we stop grouping once there are
109 no additional pairs within a δ_k of 100K. This stopping threshold of 100K results in 4,638 tornado
110 groups with 2,182 groups containing only one tornado. Also, there are 198 groups with at least
111 30 tornadoes (which we call ‘large’) with the largest group having 390 tornadoes over seven days.
112 The longest (April 22–28, 2011) event within our largest group had a duration of nine days and
113 produced 360 tornadoes. Roughly 82% of our large groups have a duration of two, three, or four
114 days. There are only nine large groups that are not multi-day events.

115 *b. Comparison of groups with well-known outbreaks*

116 We compare the tornado groups identified with our objective method with outbreaks that were
117 identified using more subjective criteria. In particular, we focus the comparison on multi-day

118 outbreaks as identified in Forbes (2004). Forbes (2004) (hereafter F04) provides a list of the top
119 25 outbreaks by number of tornadoes between 1925 and 2004. Only 13 of the outbreaks identified
120 by F04 occur after 1994; the start year of our analysis. The two lists match fairly well (Table 6).
121 We identify ten of F04's top 13 although the date ranges do not match identically. For example,
122 the May 18–19, 1995 outbreak identified by F04 is identified by our grouping from May 15–19,
123 1995. F04 identifies three outbreaks over the common period covered by both studies that are not
124 identified in our top 13 including those that occurred May 15–16, 2003, November 9–11, 2002,
125 and April 19–20, 1996. These outbreaks show up on our list ranked by number of tornadoes at
126 29, 43, and 41, respectively. We identify five groups in our top 13 that are not mentioned in F04.
127 We perfectly match the top 3 tornado outbreaks identified by Fuhrmann et al. (2014) using 100K.
128 Additionally, Schneider et al. (2004) identifies our top group (May 3 – May 11, 2003) using a
129 subjective clustering method.

130 We quantify the percent agreement between our groups and the outbreaks identified in F04
131 as follows. We count the total number of opportunities for a match as $13 + 13 = 26$. We then
132 subtract from this total the number of miss matches ($3 + 5$) and divide by the total opportunities
133 expressing the fraction as a percentage agreement. Here the agreement is $69\% [(26 - 8)/26 * 100\% = 69\%]$.
134 By varying the stopping threshold in the cluster algorithm, we change the percent
135 agreement (Fig. 1). We vary the stopping threshold in increments of 25K over the range of space-
136 time differences from 150K to 25K and find the best match with F04 in terms of percent agreement
137 at 85% when the threshold is 50K. We use 50K as the stopping threshold for further analysis
138 because it provides the best agreement with F04. This smaller space-time difference results in
139 6,899 unique groups and 137 large (at least 30 tornadoes) groups. The largest group is the April
140 26 – April 28, 2011 event that produced 292 tornadoes. The duration of the groups range from 49
141 one-day events to one five-day event. Multi-day events account for 64% of our large groups.

142 **3. Big Days in the Largest Groups**

143 Our objective is to quantify the extent to which the well-known environmental factors statisti-
144 cally explain tornado activity. Since some of the environmental factors have large diurnal fluctua-
145 tions that can confound a multi-day analysis, we reduce our focus further by considering only the
146 most prolific (big) days in these largest groups. We define the day as the 24-hour period starting at
147 6 AM local time (often referred to as the ‘convective’ day) (Doswell et al. 2006). A big convective
148 day as part of a large group is defined as one with at least ten tornadoes.

149 With this definition, we find 177 big days within our large groups. Note that there are sometimes
150 more than one big day in a single large group. Also, big days can occur within smaller groups,
151 and our set of big days accounts for only 25% of all big days in the dataset. The top two big
152 days are associated with the largest tornado group occurring on April 26, 2011 and April 27, 2011
153 (Table 2).

154 We use the May 30, 2004 as an example of a big day within a large group. The large group
155 was identified as the second most prolific by our method (and the first most prolific by Forbes
156 (2004)) and extended over a four-day period beginning on May 28th. This is the seventh biggest
157 convective day as defined by the number of tornadoes in any large group identified. Figure 2 shows
158 the genesis locations of the 88 tornadoes on that day. The gray triangle is the geographic center
159 of the set of genesis locations (centroid) and the gray polygon defines the minimum convex area
160 encompassing all locations (convex hull) on the day.

161 For each big day in a large group, we calculate the centroid from the tornado genesis locations.
162 Figure 3 shows the centroids of all 177 big days in large tornado groups with the size of the triangle
163 scaled by the number of tornadoes in the group. Most of the big days occur east of Rockies and
164 west of the Appalachians. In particular, there is a cluster of centroids across the middle South

165 extending northwestward toward the central Great Plains. There is a tendency for the biggest days
166 to occur farther east. The centroids do not have an obvious population bias.

167 A convex hull is obtained for each big day. The convex hull represents the spatial domain of
168 tornado activity on that day. Counties within the hull define the political extent of the activity and
169 we tally the number of times each county falls within (including partially) a big day hull (Figure 4).
170 Of course, larger counties will have a higher count considering all else being equal, but a pattern
171 emerges highlighting the counties over the middle South. Counties affected most often by big
172 days in large groups include those of northeastern Oklahoma eastward across southern Missouri
173 and northern Arkansas into western Kentucky and western Tennessee.

174 **4. Accumulated Tornado Energy**

175 We use tornado counts to define our tornado groups because this is what other researchers have
176 done to define outbreaks. But, our interest in this study is on the collective amount of energy all
177 the tornadoes dissipate on big days. The standard measure of tornado intensity is the Fujita and
178 Enhanced Fujita scales (Malamud and Turcotte 2012) but tornado path length and width are often
179 used to compute other intensity metrics (Brooks 2004; Fuhrmann et al. 2014; Malamud and Tur-
180 cotte 2012). Over a group of tornadoes, the Destructive Potential Index (DPI) is used as a metric
181 of the potential for damage and casualties (Thompson and Vescio 1998). Additional collective
182 measures of intensity, such as the adjusted Fujita mile, measure the outbreak strength by using the
183 EF scale rating times the path length of the tornado (Fuhrmann et al. 2014).

184 The energy dissipation (E) of a tornado estimates the potential wind energy lost at the ground.
185 It represents the potential for destruction in units of power (watts) and is calculated using damage
186 path area (A_p), air density (ρ), midpoint wind speed (v_j) for each EF rating ($j = 0, \dots, J$, where J
187 is the maximum EF rating), and the fraction of the damage path (w_j) associated with each rating

188 (Fricker et al. 2017)). Since E is an extensive variable, we sum the energy dissipation over all
 189 tornadoes occurring on a big day to get the accumulated tornado energy (ATE). Mathematically
 190 we express E and ATE as

$$E = A_p \rho \sum_{j=0}^J w_j v_j \quad (2a)$$

$$\text{ATE} = \sum_{i=1}^n E_i \quad (2b)$$

191
 192 Table 3 lists in rank order the big days in the largest groups by ATE. It includes infamous days of
 193 April 27, 2011 and May 4, 2003. ATE on April 27, 2011 is nearly four times the ATE on the next
 194 most energetic day. April 26, 2011 ranks third. Over all big days, the Spearman rank correlation
 195 between ATE and the number of tornadoes is .67 indicating a strong relationship.

196 Big days within large groups are most likely to occur during April through June with some
 197 years also showing a secondary peak after summer (Fig. 5). Monthly average ATE peaks in April
 198 followed by March and May (Table 4). Average ATE is higher during November than during
 199 May. While fewer in number, big days in large groups during November tend to produce stronger
 200 tornadoes.

201 Fig. 6 shows the time series of the annual number of big days in large groups and the annual
 202 average ATE over those days. The inter-annual variation in the number of big days is quite large
 203 ranging between two and 37, but there is no long-term trend. On the other hand, the annual average
 204 ATE appears to be increasing with the higher values occurring later in the period.

205 **5. Quantifying the Relationship Between ATE and Environmental Factors**

206 *a. NARR data*

207 Given a big day with at least ten tornadoes next we quantify the effect of known environmental
208 factors on accumulated tornado energy (ATE). To do this, we first obtain environmental data from
209 the National Climatic Data Centers (NCDC) North American Regional Reanalysis (NARR). We
210 download the 18Z NARR data for each big day. The 18Z data are chosen because tornado activity
211 generally peaks in the early afternoon. The NARR dataset ends in September 2014 so we use only
212 the big days that occur between January 1994 and September 2014. This includes 154 big days.

213 Each NARR file has 434 atmospheric variables. We consider five of them representing instability
214 and wind shear including the 0 to 180 mb CAPE and CIN (layer 375, 376), the 0 to 3000 m helicity
215 (layer 323), and the 0 to 6000 m U and V components of storm motion (layer 324, 325). We
216 compute bulk shear as the square root of the sum of the velocity components squared. We use
217 these variables because they are known to be associated with tornado development (Brown 2002;
218 Jackson and Brown 2009; Craven et al. 2002).

219 Values for each NARR variable on each big day are available as a 277 by 349 rectangular raster.
220 The corresponding big day convex hull is used as a mask, and the raster values falling under the
221 mask are composited into a single number. For the variables CAPE, bulk shear, and helicity, the
222 composite consists of taking the maximum value across all values under the mask. For CIN, the
223 composite consists of taking the minimum value. In this way, every big day value for ATE is
224 associated with each of the four environmental variables representing a spatial composite of the
225 regional scale environment in which the tornadoes occurred.

226 *b. Regression model for ATE*

227 With our sample of 154 big days, we use a regression model to quantify the relationships be-
228 tween ATE and regional scale environmental factors. A multiple regression model allows us to
229 quantify, for example, the effect of CAPE on ATE while controlling for time of year. We use
230 month as an index for time of year, and it is included in the model as a random offset to the inter-
231 cept term. Environmental variables are considered fixed effects as is year. The coefficient on year
232 is the annual trend. Values of ATE are skewed to the right with most big days having less than 5
233 TW. However, the top ten days have more than 30 TW each with the top day having more than
234 220 TW (see Table 3). The distribution of ATE on a log scale is nearly symmetric about the mean
235 value of 9 TW (Fig. 7). The median value is 3.2 TW, and the geometric mean is 2.6 TW. So, the
236 model uses the logarithm of ATE as the response variable.

237 We examine various combinations of the fixed effects and find that the best model for ATE is

$$\ln(\text{ATE}) = \beta_0 + \beta_{\text{Year}}\text{Year} + \beta_{\text{CAPE}}\text{CAPE} + \beta_{\text{Shear}}\text{Shear} + \beta_{\text{Month}}(1|\text{Month}) \quad (3)$$

238 where the coefficients for these terms are given by the corresponding β 's. Helicity and CIN do
239 not improve the model fit. The model is best in the sense that it has the lowest value of AIC. The
240 in-sample correlation between ATE and model predicted ATE is .54.

241 Model coefficients are given in Table 5. We interpret them as follows. The coefficient on the
242 year term (β_{Year}) indicates an upward trend in per big-day outbreak ATE (see Fig. 6) amounting
243 to 7% [(2.5%, 12%), 95% uncertainty (confidence) interval (UI)] per annum. Note that the percent
244 increase is calculated using $(e^{\beta_{\text{Year}}} - 1) \times 100\%$. The coefficient on the CAPE (β_{CAPE}) term
245 indicates a that for every 1000 J kg⁻¹ increase in CAPE, ATE increases by 49% [(18%, 87%),
246 95% UI] holding the other variables constant. The coefficient on the bulk shear term (β_{Shear})

247 indicates that for every $10 \text{ m}^2 \text{ s}^{-2}$ increase in the magnitude of bulk shear, ATE increases by 83%
248 [(23%, 174%), 95% UI] holding the other variables constant.

249 *c. Model residuals*

250 We compute the conditional standardized residuals (Nobre and da Motta Singer 2007) between
251 the actual and predicted values of ATE. The histogram of the residuals can be described by a
252 normal distribution, and a plot of the residuals as a function of the predicted values by month
253 shows no apparent pattern (Fig. 8) indicative of an adequate model.

254 Figure 9 shows the actual ATE versus predicted ATE for the 154 big tornado days. Lighter blue
255 points, which tend to cluster toward greater ATE, indicate more tornado casualties (deaths plus
256 direct injuries). The diagonal line indicates a perfect match between actual and predict ATE. The
257 points tend to fall along a line from lower left to upper right but with a slope less than one.

258 Big days with more ATE than predicted by the model are the points that fall to the right of
259 the diagonal line. We note that April 27, 2011 and May 22, 2004 are examples of days more
260 energetic than predicted by the model, and April 19, 2011 and May 18, 2000 are examples of days
261 less energetic than predicted by the model. Figure 10 shows the polygons defining boundaries
262 of the tornadoes on days when the model most over predicted ATE and on days when the model
263 most under predicted ATE. We see no geographic preference for big days that are under predicted
264 compared with big days that are over predicted. Further, we see no distinction in the size of the
265 areas.

266 On the other hand, the average number of tornadoes per unit area on the subset of the big days
267 that are most under predicted is 3.5 per square kilometer compared to 1.5 per square kilometer
268 on the subset of the big days that are most over predicted. This implies that the model might be

269 improved by including an environmental factor that explains the efficiency of tornado production.
270 More research on this is needed.

271 **6. Summary and List of Major Findings**

272 April 27, 2011 was the biggest day in the largest, costliest, and one of the deadliest tornado
273 outbreaks ever recorded in the United States (Knox et al. 2013). The multi-day event affected 21
274 states from Texas to New York. In this study, we first identify all big days over the period 1994–
275 2017 having ten or more tornadoes that occur in multi-day groups having 30 or more tornadoes
276 (large groups). This is done with a cluster technique on the set of space-time differences between
277 all tornadoes. Then, for each big day, we compute the accumulated tornado energy (ATE) as
278 the sum total of the energy dissipated over all tornadoes on that day. Next, we use reanalysis
279 grids to identify the extremes in CAPE, CIN, bulk shear, and helicity over the domain defined by
280 the tornado locations on these big days. A regression model is used to quantify the relationship
281 between ATE and the four environmental factors. We find an upward trend in ATE at the rate of
282 7% per annum. We also find that ATE increases significantly with additional CAPE and bulk shear
283 but not with helicity. Finally, residuals are analyzed to diagnose model adequacy and to identify
284 the largest under and over predictions.

285 The major findings are:

- 286 • An objective cluster technique can reliably identify tornado outbreaks.
- 287 • Accumulated tornado energy is a useful metric of outbreak severity.
- 288 • Outbreak severity increases by 49% for every 1000 J kg^{-1} increase in CAPE.
- 289 • Outbreak severity increases by 83% for every $10 \text{ m}^2\text{s}^{-2}$ increase in bulk shear.

290 The study is limited by sample size (only 154 big day cases) and by an exclusive focus on the
291 last 20 years of a much longer tornado record. The study could be improved by considering more
292 cases from the earlier years. The cost of including earlier data would be greater uncertainty on
293 the estimates of per-tornado energy dissipation. The study might also be improved by including
294 other environmental factors in the model, especially ones that are related to the efficiency of tor-
295 nado production. Future work will examine the spatial variation in the factors affecting outbreak
296 severity and quantify the relationship between outbreak casualties and the environmental factors
297 controlling for how many people were within the outbreak area.

298 *Acknowledgments.* The code used to produce the results of this paper is available at [https:](https://github.com/jelsner/tor-clusters)
299 [//github.com/jelsner/tor-clusters](https://github.com/jelsner/tor-clusters).

300 **References**

- 301 American Meteorological Society, cited 2018: Tornado Outbreak, Glossary of Meteorology.
302 [Available online at <http://glossary.ametsoc.org/wiki/Citation>].
- 303 Bates, D., M. Mächler, B. Bolker, and S. Walker, 2015: Fitting linear mixed-effects models using
304 lme4. *Journal of Statistical Software*, **67** (1), 1–48, doi:10.18637/jss.v067.i01.
- 305 Birant, D., and A. Kut, 2007: ST-DBSCAN: An algorithm for clustering spatial–temporal data.
306 *Data & Knowledge Engineering*, **60** (1), 208–221, doi:10.1016/j.datak.2006.01.013.
- 307 Brooks, H. E., 2004: On the relationship of tornado path length and width to intensity. *Weather
308 and Forecasting*, **19**, 310–319.
- 309 Brooks, H. E., C. A. Doswell, and J. Cooper, 1994: On the environments of tornadic and nontor-
310 nadic mesocyclones. *Weather and Forecasting*, **9**, 606–618, doi:10.1175/1520-0434.
- 311 Brown, M., 2002: The spatial, temporal, and thermodynamic characteristics of Southern-Atlantic
312 United States tornado events. *Physical Geography*, **23** (5), 401–417, doi:10.2747/0272-3646.
313 23.5.401.
- 314 Concannon, P., H. E. Brooks, and C. A. Doswell, 2000: Climatological risk of strong and violent
315 tornadoes in the United States. *Second Conference on Environmental Applications*.
- 316 Craven, J. P., R. E. Jewell, and H. E. Brooks, 2002: Comparison between observed convective
317 cloud-base heights and lifting condensation level for two different lifted parcels. *Weather and
318 Forecasting*, **17** (4), 885–890, doi:10.1175/1520-0434(2002)017<0885:CBOCCB>2.0.CO;2.
- 319 Dean, A. R., 2010: P2.19 An analysis of clustered tornado events. *25th Conference on Severe
320 Local Storms*.

321 Doswell, C. A., R. Edwards, R. L. Thompson, J. A. Hart, and K. C. Crosbie, 2006: A simple and
322 flexible method for ranking severe weather events. *Weather and Forecasting*, **21** (6), 939–951,
323 doi:10.1175/waf959.1, URL <https://doi.org/10.1175/waf959.1>.

324 Forbes, G. S., 2004: Meteorological aspects of high-impact tornado outbreaks. Preprints, *22nd*
325 *Conf. on Severe Local Storms*, Hyannis, MA, Amer. Meteor. Soc., 1–12.

326 Fricker, T., J. B. Elsner, and T. H. Jagger, 2017: Population and energy elasticity of tornado
327 casualties. *Geophysical Research Letters*, **44**, 3941–3949, doi:10.1002/2017GL073093.

328 Fuhrmann, C. M., C. E. Konrad II, M. M. Kovach, J. T. McLeod, W. G. Schmitz, and P. G.
329 Dixon, 2014: Ranking of tornado outbreaks across the United States and their climatological
330 characteristics. *Weather and Forecasting*, **29**, 684–701.

331 Galway, J. G., 1977: Some climatological aspects of tornado outbreaks. *Monthly Weather Review*,
332 **105**, 477–484.

333 Jackson, J. D., and M. E. Brown, 2009: Sounding-derived low-level thermodynamic characteris-
334 tics associated with tornadic and non-tornadic supercell environments in the Southeast United
335 States. *National Weather Digest*, **33**, 16–26.

336 Johns, R. H., J. M. Davies, and P. W. Leftwich, 1993: Some wind and instability parameters
337 associated with strong and violent tornadoes: 2. Variations in the combinations of wind and
338 instability parameters. *Washington DC American Geophysical Union Geophysical Monograph*
339 *Series*, **79**, 583–590, doi:10.1029/GM079p0583.

340 Knox, J. A., and Coauthors, 2013: Tornado debris characteristics and trajectories during the 27
341 april 2011 super outbreak as determined using social media data. *Bulletin of the American Me-*
342 *teorological Society*, **94** (9), 1371–1380, doi:10.1175/bams-d-12-00036.1.

- 343 Knupp, K. R., and Coauthors, 2014: Meteorological overview of the devastating 27 april 2011
344 tornado outbreak. *Bulletin of the American Meteorological Society*, **95** (7), 1041–1062.
- 345 Korotky, W., R. W. Przybylinski, and J. A. Hart, 1993: The Plainfield, Illinois, tornado of August
346 28, 1990: The evolution of synoptic and mesoscale environments. *Washington DC American*
347 *Geophysical Union Geophysical Monograph Series*, **79**, 611–624, doi:10.1029/GM079p0611.
- 348 Malamud, B. D., and D. L. Turcotte, 2012: Statistics of severe tornadoes and severe tornado
349 outbreaks. *Atmospheric Chemistry and Physics*, **12** (18), 8459–8473.
- 350 Malamud, B. D., D. L. Turcotte, and H. E. Brooks, 2016: Spatial-temporal clustering of tornadoes.
351 *Natural Hazards and Earth System Sciences*, **16**, 2823–2834, doi:10.5194/nhess-16-2823-2016.
- 352 Nobre, J. S., and J. da Motta Singer, 2007: Residual analysis for linear mixed models. *Biometri-*
353 *cal Journal*, **49** (6), 875–875, doi:10.1002/bimj.200790008, URL [https://doi.org/10.1002/bimj.](https://doi.org/10.1002/bimj.200790008)
354 200790008.
- 355 Schneider, R. S., H. E. Brooks, and J. T. Schafer, 2004: Tornado outbreak day sequences: Historic
356 events and climatology (1875–2003). Preprints,, *22nd Conf. on Severe Local Storms*, Hyannis,
357 MA, Amer. Meteor. Soc., 1–11.
- 358 Thompson, R., and M. Vescio, 1998: The Destruction Potential Index - A method for comparing
359 tornado days. *19th Conference on Severe Local Storms*.

360 **LIST OF TABLES**

361 **Table 1.** Top 13 tornado groups and outbreaks over the common period of analysis using
362 100K space-time units as the cutoff threshold for including tornadoes. 20

363 **Table 2.** The top ten big days in the largest tornado groups. 21

364 **Table 3.** Top ten convective days ranked by accumulated tornado energy (ATE) in units
365 of terawatts (TW). 22

366 **Table 4.** Seasonal variation in ATE (TW), number of tornadoes, and number of prolific
367 days by month. The number of tornadoes and number of big days are based on
368 the period 1994–2017. 23

369 **Table 5.** Coefficient estimates from a regression model of ATE onto year, CAPE, and
370 shear using data from $n = 154$ big days in large groups over the period January
371 1994 through September 2014. Std. Error is the standard error of the estimate
372 and the t value is the ratio of the estimate to the standard error. The coefficients
373 were determined via an iterative maximum likelihood approach with the `lmer`
374 function from the `lme4` package for R (Bates et al. 2015). 24

Our Top 13 Groups	Forbes' Top 13 Outbreaks
May 3–11, 2003	May 29–31, 2004
May 28–31, 2004	January 21–22, 1999
January 21–22, 1999	May 3–4, 1999
May 2–4, 1999	May 6–8, 2003
May 15–19, 1995	May 4–5, 2003
June 22–24, 2003	September 5–8, 2004
June 3–6, 1999	June 24, 2003
September 15–18, 2004	November 23–24, 2004
April 25–28, 1994	May 9–11, 2003
May 24–28, 1997	May 15–16, 2003
November 22–24, 2004	November 9–11, 2002
September 4–8, 2004	April 19–20, 1996
May 30–June 2, 1998	May 18–19, 1995

375 TABLE 1. Top 13 tornado groups and outbreaks over the common period of analysis using 100K space-time
376 units as the cutoff threshold for including tornadoes.

Convective Day	Number of Tornadoes	Number of Casualties
April 27, 2011	173	3069
April 26, 2011	103	97
January 21, 1999	99	171
June 24, 2003	94	12
May 5, 2007	90	24
May 25, 2011	90	23
May 30, 2004	88	46
May 4, 2003	86	384
February 5, 2008	85	482
April 14, 2012	84	79

TABLE 2. The top ten big days in the largest tornado groups.

Convective Day	ATE (TW)
April 27, 2011	221
April 24, 2010	64
April 26, 2011	46
May 24, 2011	43
February 5, 2008	39
March 2, 2012	38
May 10, 2010	34
April 14, 2012	32
May 4, 2003	31
May 22, 2004	30

TABLE 3. Top ten convective days ranked by accumulated tornado energy (ATE) in units of terawatts (TW).

Month	Average ATE (TW)	Number of Tornadoes	Number of Big Days
January	4.07	345	7
February	7.89	321	9
March	13.53	427	10
April	16.24	1696	37
May	8.92	2220	49
June	4.10	729	18
July	0.63	43	2
August	1.47	71	2
September	1.01	458	16
October	2.28	261	8
November	8.11	587	14
December	5.59	123	5

377 TABLE 4. Seasonal variation in ATE (TW), number of tornadoes, and number of prolific days by month. The
378 number of tornadoes and number of big days are based on the period 1994–2017.

	Estimate	Std. Error	<i>t</i> value
β_0	25.609	0.656	39.060
β_{Year}	0.079	0.022	3.520
β_{CAPE}	0.396	0.118	3.355
β_{Shear}	0.606	0.205	2.954

379 TABLE 5. Coefficient estimates from a regression model of ATE onto year, CAPE, and shear using data from n
380 = 154 big days in large groups over the period January 1994 through September 2014. Std. Error is the standard
381 error of the estimate and the t value is the ratio of the estimate to the standard error. The coefficients were
382 determined via an iterative maximum likelihood approach with the `lmer` function from the `lme4` package for R
383 (Bates et al. 2015).

LIST OF FIGURES

384

385 **Fig. 1.** Percent agreement between our tornado groups and the tornado outbreaks identified in
386 Forbes (2004). 26

387 **Fig. 2.** The May 30, 2004 big tornado day is characterized by 88 tornadoes. Each dot represents
388 a tornado genesis location, and the triangle is the geographic center of the genesis loca-
389 tion. The dark gray line defines the minimum convex polygon around the genesis locations
390 (convex hull). 27

391 **Fig. 3.** Centroids of genesis locations occurring on big days in large groups. The triangles are sized
392 by the number of tornadoes on that day. 28

393 **Fig. 4.** Big Day density by county. 29

394 **Fig. 5.** Accumulated tornado energy (ATE) by day of year on days with more than ten tornadoes
395 occurring within large groups of at least 30 tornadoes, 1994–2017. Tic labels on the x-axis
396 are the start day of each month. 30

397 **Fig. 6.** Number of big days by year, 1994–2017. Points are sized by annual average ATE. 31

398 **Fig. 7.** Histogram of per big day ATE, 1994–2017. The horizontal axis is on a log scale. 32

399 **Fig. 8.** Conditional standardized residuals from the linear regression model. (A) Histogram and (B)
400 Residuals as a function of predicted values of ATE. 33

401 **Fig. 9.** Actual versus predicted accumulated tornado energy (ATE) for the $n = 154$ big tornado days.
402 The predicted are based on the regression model (Eq. 3). The color shading from dark to
403 light indicates increasing number of casualties. 34

404 **Fig. 10.** Areas defining the boundary of all tornadoes on big days. Days selected are those where the
405 model most over predicted (blue) and most under predicted (pink) ATE. 35

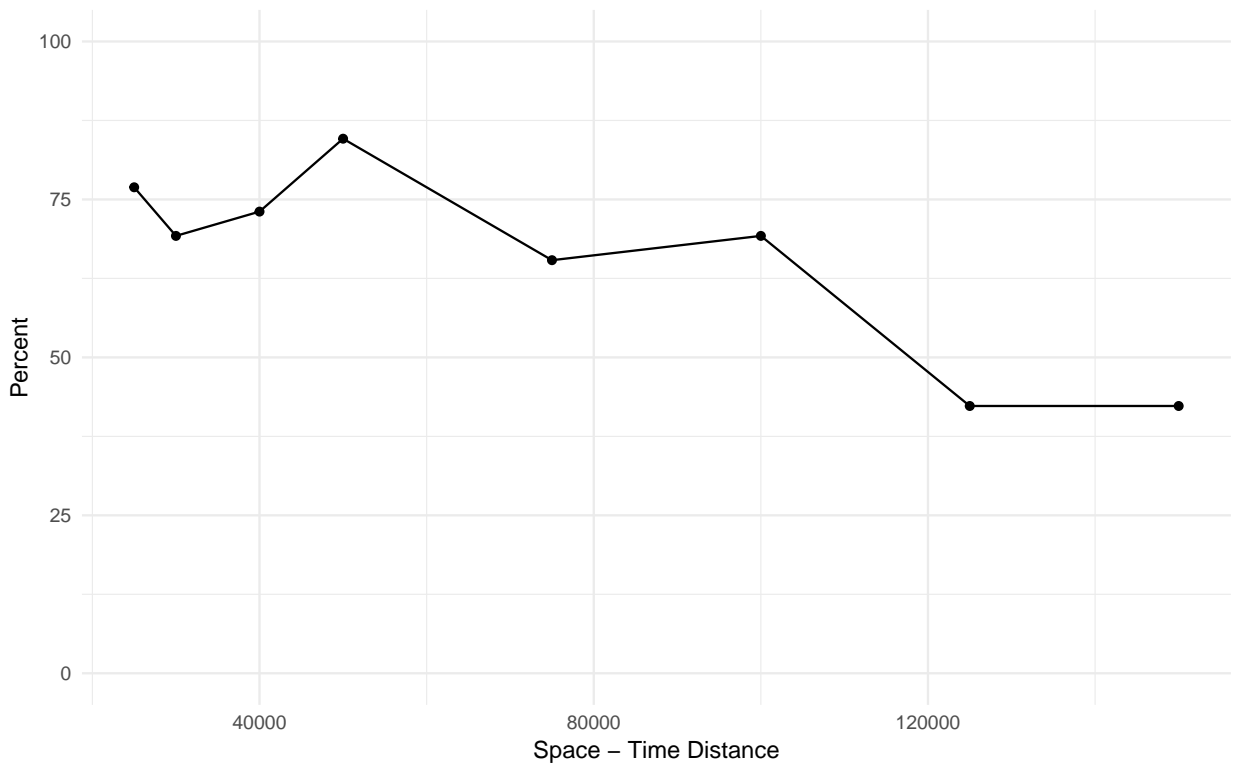
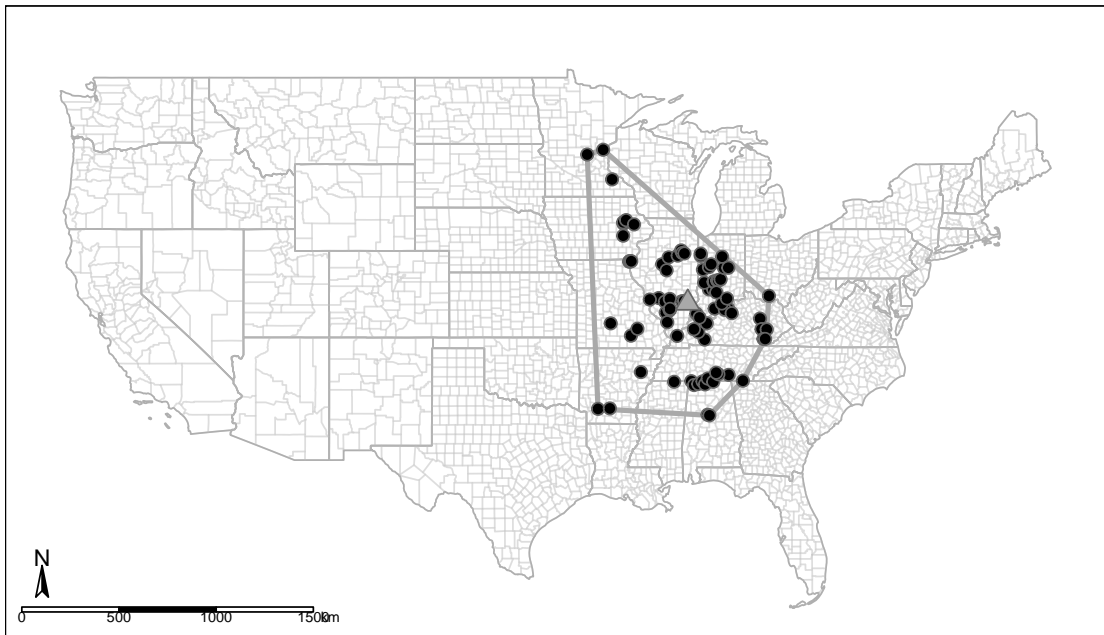
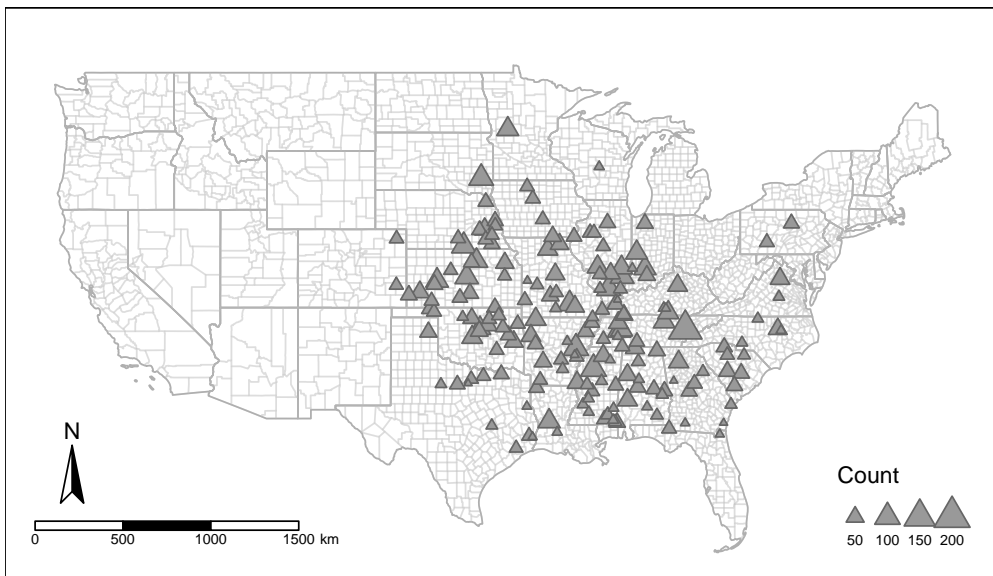


FIG. 1. Percent agreement between our tornado groups and the tornado outbreaks identified in Forbes (2004).



406 FIG. 2. The May 30, 2004 big tornado day is characterized by 88 tornadoes. Each dot represents a tornado
407 genesis location, and the triangle is the geographic center of the genesis location. The dark gray line defines the
408 minimum convex polygon around the genesis locations (convex hull).



409 FIG. 3. Centroids of genesis locations occurring on big days in large groups. The triangles are sized by the
410 number of tornadoes on that day.

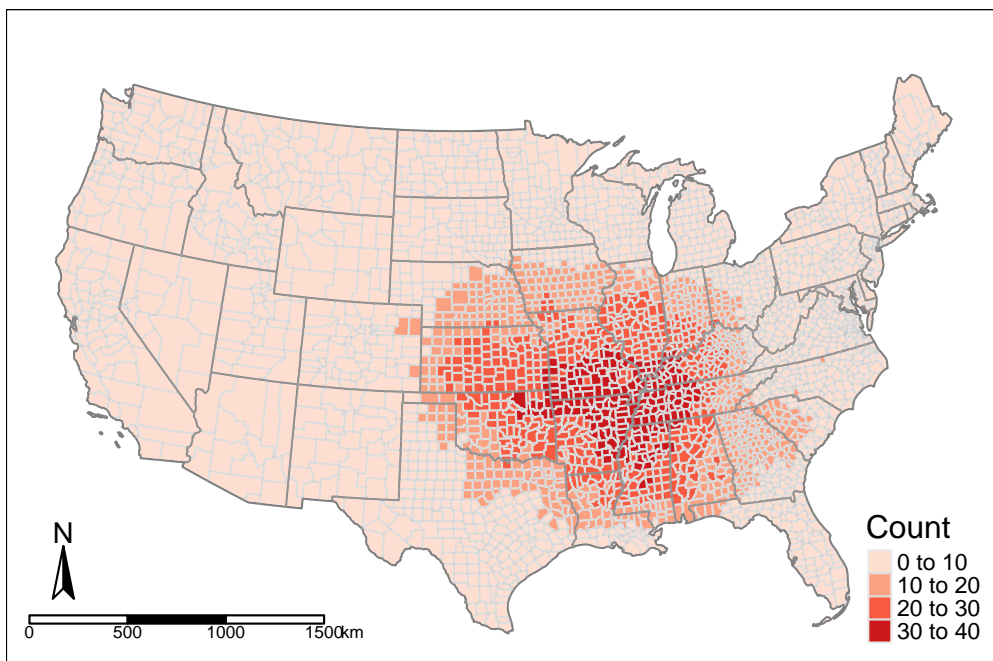
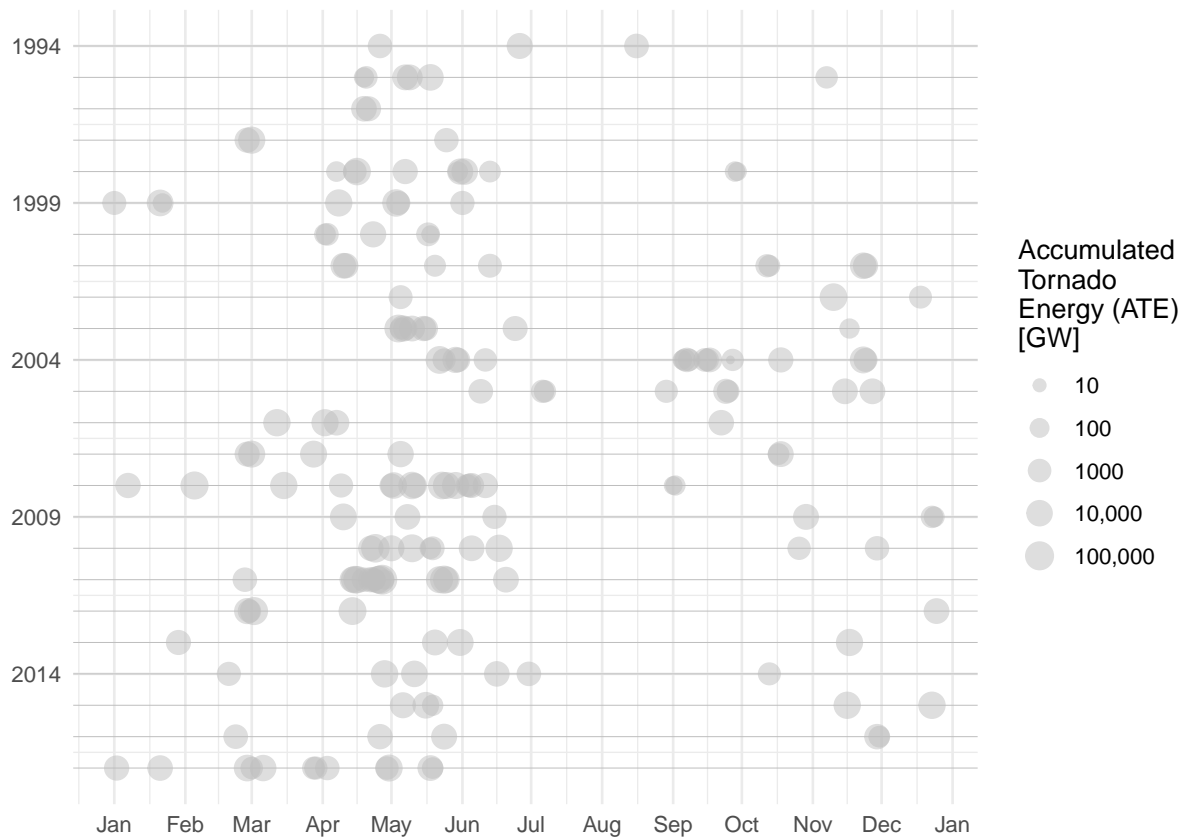


FIG. 4. Big Day density by county.



411 FIG. 5. Accumulated tornado energy (ATE) by day of year on days with more than ten tornadoes occurring
 412 within large groups of at least 30 tornadoes, 1994–2017. Tic labels on the x-axis are the start day of each month.

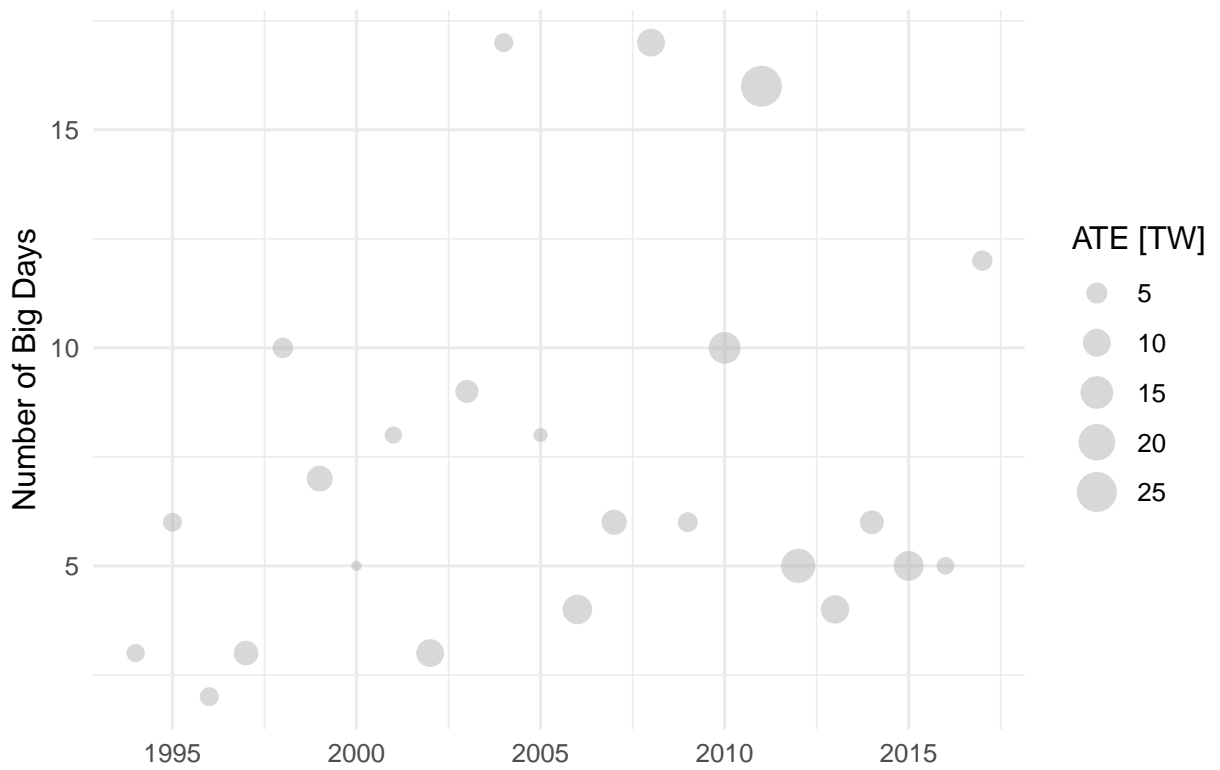


FIG. 6. Number of big days by year, 1994–2017. Points are sized by annual average ATE.

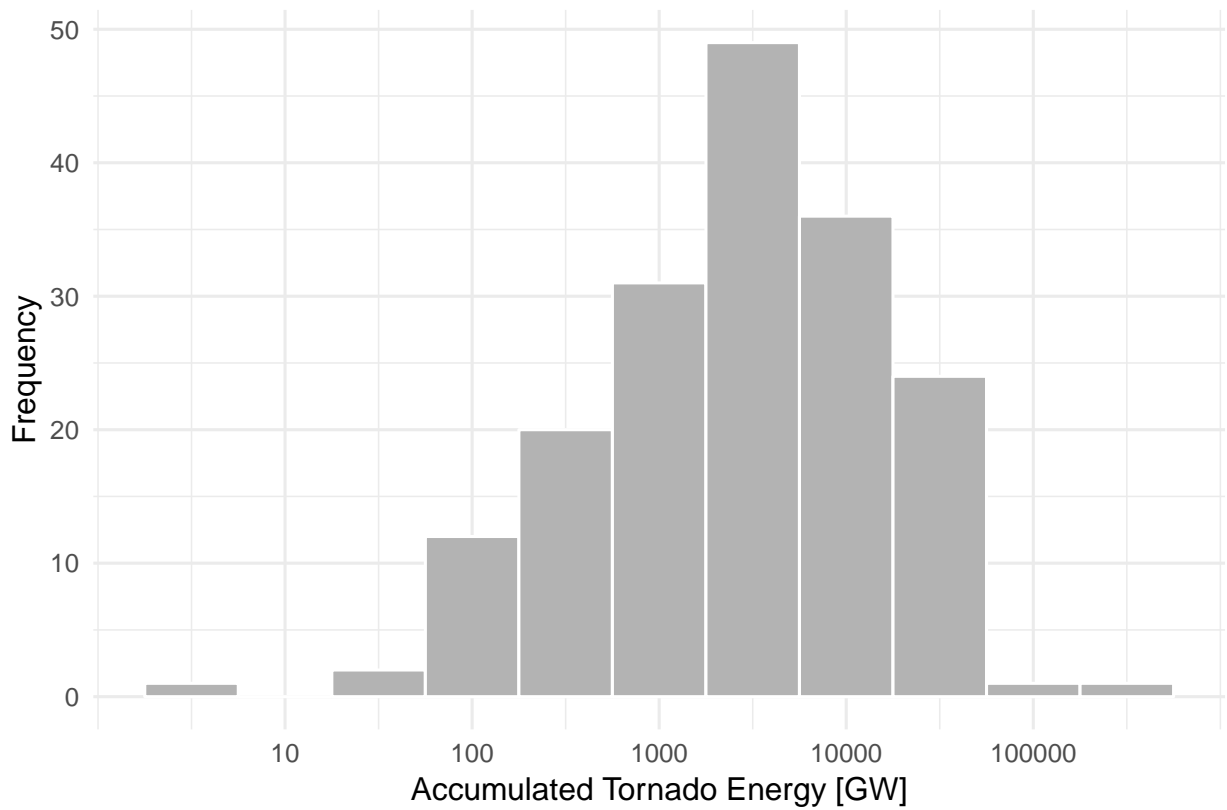
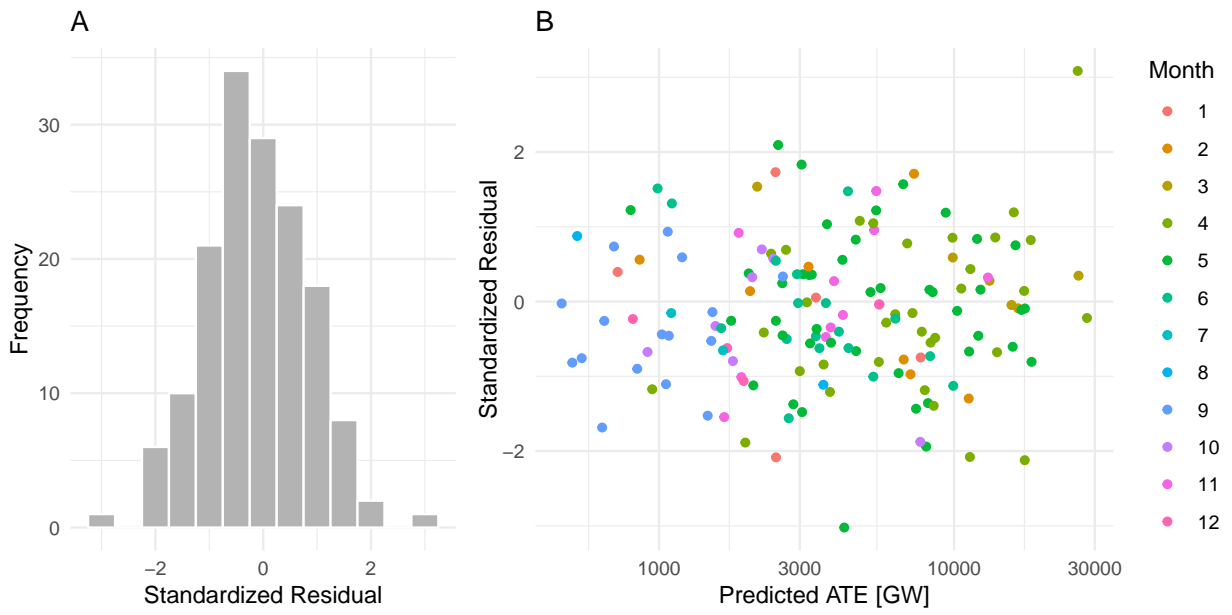
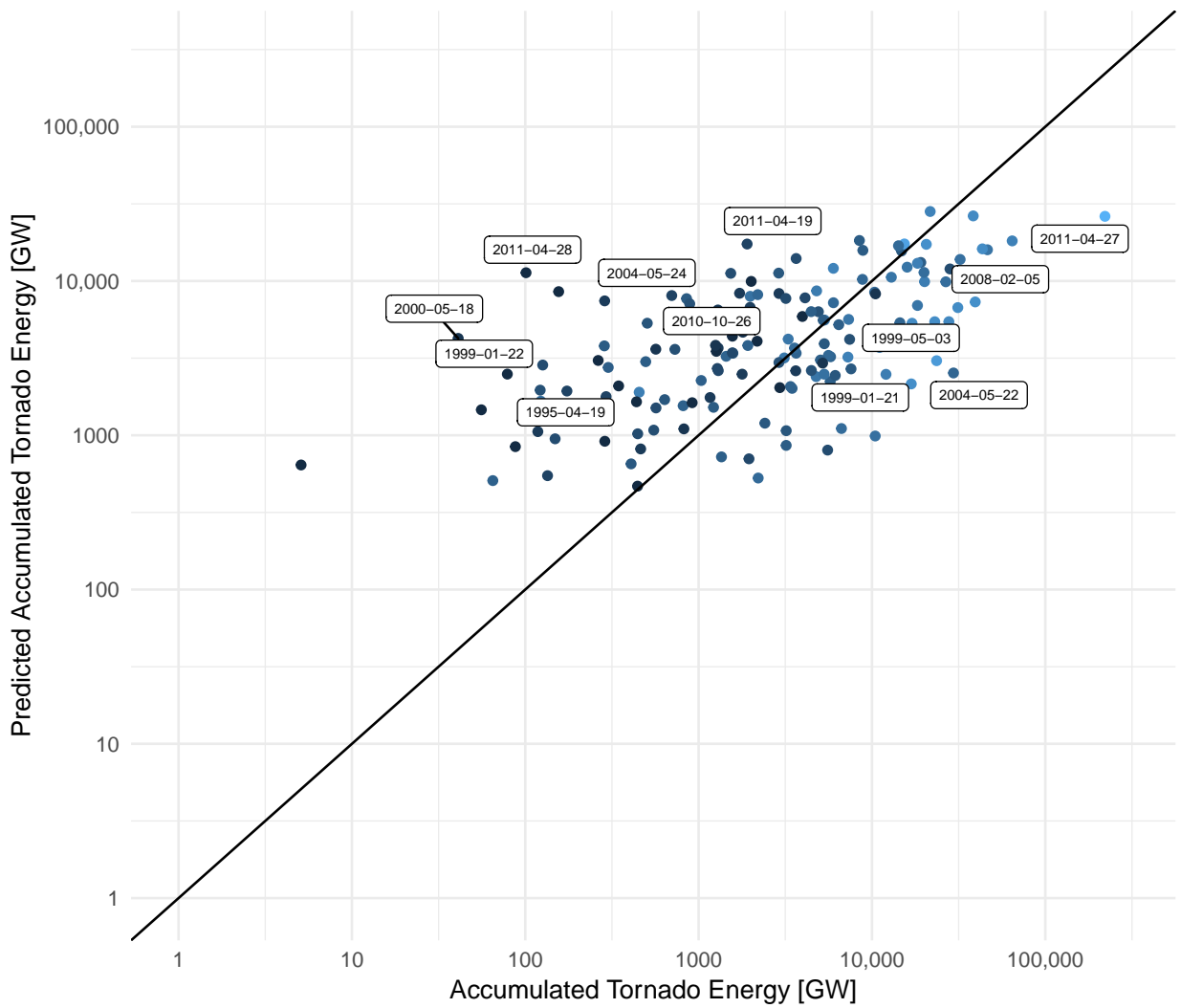


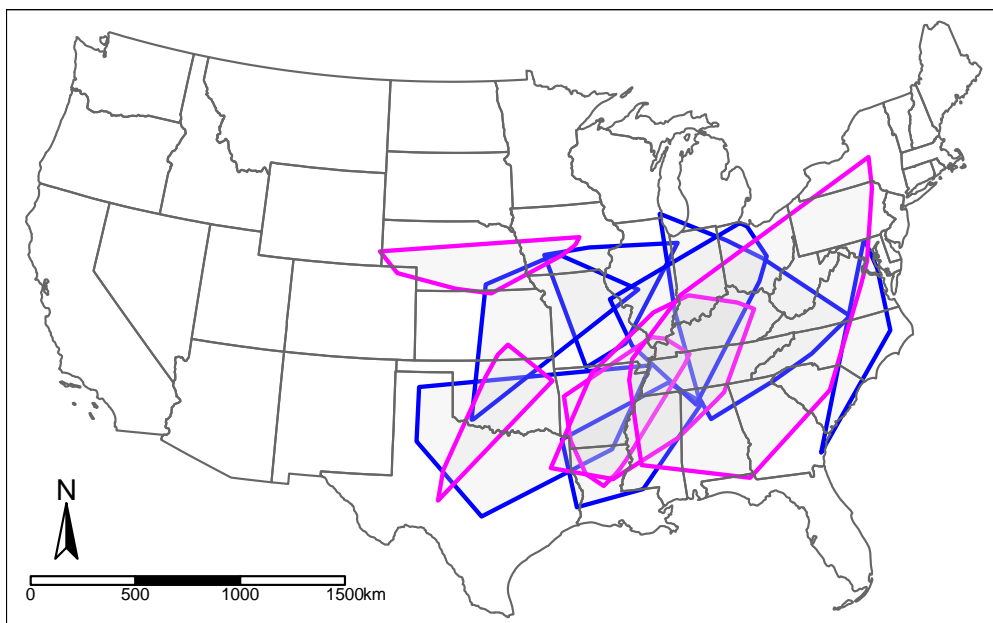
FIG. 7. Histogram of per big day ATE, 1994–2017. The horizontal axis is on a log scale.



413 FIG. 8. Conditional standardized residuals from the linear regression model. (A) Histogram and (B) Residuals
 414 as a function of predicted values of ATE.



415 FIG. 9. Actual versus predicted accumulated tornado energy (ATE) for the $n = 154$ big tornado days. The
 416 predicted are based on the regression model (Eq. 3). The color shading from dark to light indicates increasing
 417 number of casualties.



418 FIG. 10. Areas defining the boundary of all tornadoes on big days. Days selected are those where the model
419 most over predicted (blue) and most under predicted (pink) ATE.